



Theoretical study of kinetic isotope effects for vacancy diffusion of impurity in solids

Yuxi Jing¹ · Xuefang Li^{1,2,3} · Yun Liu^{1,2,3}

Received: 9 April 2024 / Revised: 8 May 2024 / Accepted: 21 May 2024 / Published online: 13 June 2024

© The Author(s), under exclusive licence to Science Press and Institute of Geochemistry, CAS and Springer-Verlag GmbH Germany, part of Springer Nature 2024

Abstract Theoretical studies of the diffusional isotope effect in solids are still stuck in the 1960s and 1970s. With the development of high spatial resolution mass spectrometers, isotopic data of mineral grains are rapidly accumulated. To dig up information from these data, molecular-level theoretical models are urgently needed. Based on the microscopic definition of the diffusion coefficient (D), a new theoretical framework for calculating the diffusional isotope effect ($\text{DIE}_{(v)}$) (in terms of D^*/D) for vacancy-mediated impurity diffusion in solids is provided based on statistical mechanics formalism. The newly derived equation shows that the $\text{DIE}_{(v)}$ can be easily calculated as long as the vibration frequencies of isotope-substituted solids are obtained. The calculated $\text{DIE}_{(v)}$ values of $^{199}\text{Au}/^{195}\text{Au}$ and $^{60}\text{Co}/^{57}\text{Co}$ during diffusion in Cu and Au metals are all within 1% of errors compared to the experimental data, which shows that this theoretical model is reasonable and precise.

Keywords Vacancy diffusion · Diffusional isotope effect · Statistical mechanics

1 Introduction

In solids, diffusion is the only way for atoms to migrate. Isotopes of the same element have small differences in their migration rates because of their mass. This phenomenon is called the diffusion isotope effect (DIE). The DIE can lead to kinetic isotope fractionation along the grain profiles of solids. The study of DIE in solids can therefore help us understand the mechanisms of diffusion in solids. The DIE can also be used to study ionic conductivity (Kalyagin et al. 2008) and to enrich certain isotopes (Morita and Hoshino 2020) in the field of materials science. In geosciences, the study of the DIE is the basis of diffusional chronology, and it has the potential to provide thermal history information under high time resolution for geologic processes (Zhang and Cherniak 2010).

With the development of mass spectrometers with high spatial resolution, data on isotopic compositions at the particle/grain scale have rapidly accumulated (Trull and Kurz 1993; Mueller et al. 2014; Richter et al. 2014), but the interpretation of those data is still insufficient due to the lack of theoretical models. The DIE is usually expressed as the ratio of the diffusion coefficient (D^*/D) ($*$ denotes the one involving heavy isotopes for all symbols in this study). The theoretical treatment of DIE has remained at the same level as in the 1960s and 1970s. However, classical diffusion theory, which is based on classical transition state theory (TST) (Eyring 1935), employs many approximations and assumptions, e.g., the one-atom hypothesis (Wert and Zener 1949; Wert 1950), the high-temperature approximation relation (Vineyard 1957; Le Claire 1966), and the neglect of quantum effects (Kobayashi and Hoshino 2018). These approximations can lead to large errors in the calculation of DIEs, especially at room or not high temperatures. Li et al. (2023) evaluated

✉ Xuefang Li
lixuefang@cdu.edu.cn

✉ Yun Liu
liuyun@vip.gyig.ac.cn

¹ Research Center for Planetary Science, College of Earth and Planetary Sciences, Chengdu University of Technology, Chengdu 610059, China

² State Key Laboratory of Ore Deposit Geochemistry, Institute of Geochemistry, Chinese Academy of Sciences, Guiyang 550081, China

³ CAS Center for Excellence in Comparative Planetology, Hefei 230026, China

these approximations. They considered quantum effects and provided a proper method for calculating the DIE for diffusion in solids with the interstitial mechanism.

Similarly, these approximations and assumptions can also influence the $DIE_{(v)}$ for vacancy diffusion, which is the most common form of diffusion in minerals. Therefore, a higher-level theoretical method for determining the isotope effect of vacancy diffusion is needed. In this study, starting from the microscopic expression of the diffusion coefficient (D), a new $DIE_{(v)}$ calculation equation under the vacancy diffusion of impurity atoms in solids is provided based on quantum mechanics and statistical thermodynamics. Then, the calculated $DIE_{(v)}$ of the four systems, which have well-constrained experimental data, are compared with the experimental data to check the reliability of this new method.

2 Methods

In this study, self-diffusion refers to the diffusion process of principal atom A in solvent atom A; tracer diffusion refers to the diffusion process of isotope A* of principal atom A in solvent atom A; and impurity diffusion is also called solute diffusion and refers to the diffusion process of impurity X with a very low concentration in solvent atom A (Philibert 1991). Because the atoms of interest in this study are A*, X and their isotope X*, whose masses are different from that of A, they are collectively referred to as impurity atoms. This study focuses on the vacancy diffusion of impurity atoms, which can also be called vacancy-mediated impurity diffusion.

In solids, diffusion is accomplished by the migration of defects. Defects in solids include point defects, line defects, and plane defects. This work involves the diffusion of point defects (impurities or vacancies) inside solids, where atoms migrate by the continuous jumps of defects. Vacancy diffusion is the process of impurity atoms jumping into the nearest neighboring vacancies. In the random walk theory, the impurity atom diffuses with a monovacancy mechanism, and the microscopic expression of D is (Mehrer 2007):

$$D = a^2 \Gamma f \tag{1}$$

a is the lattice parameter, and f is the correlation coefficient, indicating the degree of deviation from the random walk in two successive jumps. In the interstitial diffusion mechanism, there is no correlation between successive jumps, i.e., $f=1$; for the vacancy diffusion mechanism, there is usually a correlation between them, $f < 1$ (Mehrer 2007). Γ is the jump rate of the impurity atom to the adjacent vacancy and represents the number of atom jumps (n) per unit of time (t). For different isotopes, a is the same, therefore:

$$\frac{D^*}{D} = \frac{\Gamma^* f^*}{\Gamma f} \tag{2}$$

The most essential formula for f was suggested as follows (Bardeen and Herring 1952):

$$f = 1 + \frac{2}{n} \sum_{i=1}^{n-1} \sum_{j=1}^{n-i} \overline{\cos\theta_{i,i+j}} \tag{3}$$

Here, n is the number of atom jumps in a cubic lattice, and θ is the angle between two successive jumps (i, j), therefore, f only depends on the angle θ . Under completely random conditions, $\sum_{i=1}^{n-1} \sum_{j=1}^{n-i} \cos\theta_{i,i+j} = 0$, but vacancy diffusion is not completely random, which means that $\sum_{i=1}^{n-1} \sum_{j=1}^{n-i} \cos\theta_{i,i+j} \neq 0$. It has been shown (Jing 2022) that the θ between two jumps for the impurity atoms is related to the exchange mechanism between vacancy and solvent atoms, which is related to the binding energy between them, and it is independent of the isotope mass of the impurity atoms. As a result, the θ values for the isotopes of impurity atoms are the same, and the ratio f^*/f is 1. This demonstrates that the effect of f cannot be ignored when analyzing the absolute value of D for vacancy diffusion. Therefore, when the impurity concentration and vacancy concentration are very low, the effect of f^*/f can be neglected, and $DIE_{(v)}$ can be expressed as,

$$\frac{D^*}{D} = \frac{\Gamma^*}{\Gamma} \tag{4}$$

In vacancy-mediated self-diffusion, Γ , in which an atom jumps to a given vacancy, can be expressed as

$$\Gamma = w C_{1V}^{eq} \tag{5}$$

where, w is the exchange frequency between a jumping atom and a vacancy, and C_{1V}^{eq} represents the probability of forming a vacancy in the crystal at thermodynamic equilibrium. In statistical thermodynamics at thermal equilibrium, C_{1V}^{eq} is obtained by (Mehrer 2007)

$$C_{1V}^{eq} = \exp\left(-\frac{\Delta G_{1V}^f}{k_B T}\right) \tag{6}$$

where, ΔG_{1V}^f is the Gibbs free energy of forming only one vacancy (V) in a perfect crystal. k_B is the Boltzmann constant, and T is the Kelvin temperature.

For vacancy-mediated impurity diffusion, we must consider attractive or repulsive interactions between impurity atoms and vacancies. We need to recalibrate the probability P of forming a vacancy in the nearest neighbor position of the impurity (X). The difference between the probability P

and the probability C_{1V}^{eq} is the Gibbs free energy of binding ΔG_{X-V}^B for the impurity-vacancy pair (X-V). For $\Delta G_{X-V}^B > 0$ ($\Delta G_{X-V}^B < 0$), P is enhanced (reduced) concerning C_{1V}^{eq} . P is given by the Lomer equation (Lomer 1958):

$$P = C_{1V}^{eq} \exp\left(\frac{\Delta G_{X-V}^B}{k_B T}\right) = \exp\left(-\frac{\Delta G_{1V}^F}{k_B T}\right) \exp\left(\frac{\Delta G_{X-V}^B}{k_B T}\right) \quad (7)$$

Thus, we can obtain the jump rate Γ of impurity atoms for vacancy-mediated impurity diffusion,

$$\Gamma = w C_{1V}^{eq} \exp\left(\frac{\Delta G_{X-V}^B}{k_B T}\right) = w \Delta \exp\left(-\frac{\Delta G_{1V}^F}{k_B T}\right) \exp\left(\frac{\Delta G_{X-V}^B}{k_B T}\right) \quad (8)$$

Therefore, $DIE_{(v)}$ is

$$\frac{D^*}{D} = \frac{\Gamma^*}{\Gamma} = \frac{w^* \exp\left(-\frac{\Delta G_{1V}^F}{k_B T}\right)^* \exp\left(\frac{\Delta G_{X-V}^B}{k_B T}\right)^*}{w \exp\left(-\frac{\Delta G_{1V}^F}{k_B T}\right) \exp\left(\frac{\Delta G_{X-V}^B}{k_B T}\right)} \quad (9)$$

The $DIE_{(v)}$ will then be split into three sections according to the right-hand side of Eq. (9), each of which will be discussed below.

2.1 Exchange frequency (w)

The TST was used to address the jump of atoms from one position to another in solids, and this jump needed to cross an energy barrier. Wert and Zener (1949) suggested that w can be expressed as

$$w = v^0 \exp\left(-\frac{\Delta G^M}{k_B T}\right) \quad (10)$$

where v^0 is the attempt frequency of the jumping atom, and ΔG^M is the Gibbs free energy of the jumping atom migration (the energy difference between the transition state and the initial state). When interstitial diffusion occurs, the interstitial position itself is present, and no formation energy is needed. Hence, the probability of forming an interstitial adjacent to the jumping atom is 1. This means that only w needs to be considered when calculating Γ . For interstitial diffusion, the DIE (D^*/D) equals the ratio of the exchange frequency (w^*/w).

Under the classical limit, w^*/w is reduced to the classical rate theory (Vineyard 1957; Schoen 1958) and is given as

$$\frac{w^*}{w} \cong \sqrt{\frac{m}{m^*}} \quad (11)$$

However, it includes several approximations, such as the one-atom hypothesis and the high-temperature approximation, which can lead to large errors in the calculations,

especially at low temperatures. Li et al. (2023) improved the TST to reconstruct the theoretical derivation of w , modified the approximation of previous theories and quantum effects, and obtained an improved equation for w in solids:

$$w = v^{TS} \left(\frac{Q_{vib}^{TS}}{Q_{vib}^{IS}}\right) \exp\left(-\frac{\Delta E_{elec}}{k_B T}\right) \exp\left(-\frac{\Delta(PV)}{k_B T}\right) \quad (12)$$

v^{TS} is the imaginary vibrational frequency of the TS, and Q_{vib} is the vibrational partition function. For the ratio of w for heavy and light isotopes,

$$\frac{w^*}{w} = \left(\frac{v^*}{v}\right)^{TS} \frac{\left(\frac{Q_{vib}^*}{Q_{vib}}\right)^{TS}}{\left(\frac{Q_{vib}^*}{Q_{vib}}\right)^{IS}} \exp\left(-\frac{\Delta \Delta E_{elec}}{k_B T}\right) \exp\left(-\frac{\Delta \Delta(PV)}{k_B T}\right) \quad (13)$$

Which

$$\Delta \Delta E_{elec} = (E_{elec}^* - E_{elec})^{TS} - (E_{elec}^* - E_{elec})^{IS} \quad (14)$$

$$\Delta \Delta(PV) = (P^* V^* - PV)^{TS} - (P^* V^* - PV)^{IS} \quad (15)$$

Based on the Born–Oppenheimer approximation (BOA), the difference in electron energy E_{elec} and volume work PV is considered to be 0 before and after the light and heavy isotopes are replaced. Equation (13) can also be used for vacancy-mediated impurity diffusion, therefore, we obtain

$$\frac{w^*}{w} = \left(\frac{v^*}{v}\right)_{X-V}^{TS} \frac{\left(\frac{Q_{vib}^*}{Q_{vib}}\right)_{X-V}^{TS}}{\left(\frac{Q_{vib}^*}{Q_{vib}}\right)_{X-V}^{IS}} \quad (16)$$

A schematic diagram of the energy items in Eq. (16) is shown in Fig. 1a.

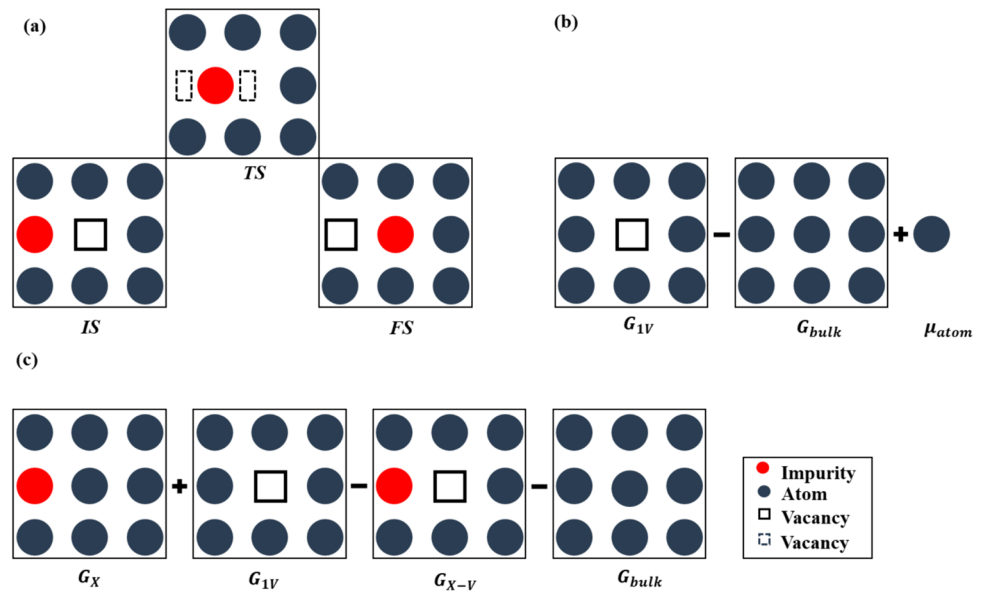
2.2 Vacancy formation Gibbs free energy (ΔG_{1V}^F)

The Gibbs free energy of formation (ΔG_D^F) of defects (impurities or vacancies) in the charge state (q) is defined as (Van de Walle and Neugebauer 2004)

$$\Delta G_D^F = G_D - G_{bulk} - \sum n_i \mu_i + q(G_{Fermi} + G_v + \gamma) \quad (17)$$

G_D is the Gibbs free energy for a crystal containing defects, G_{bulk} is the Gibbs free energy for a perfect crystal without any defects, n_i represents the number of atoms (host atoms or impurity atoms) that have been added to ($n_i > 0$) or removed from ($n_i < 0$) the supercell when the defect is created, and μ_i is the corresponding chemical potential of the atom. G_{Fermi} is the Fermi level, G_v is the Gibbs free energy of the bulk valence-band maximum, γ is a correction term, and

Fig. 1 **a** Schematic diagram of vacancy-mediated impurity jump. The left, middle and right of this figure correspond to the initial state (*IS*), the transition state (*TS*), and the final state (*FS*), respectively. **b** Physical image of the vacancy formation Gibbs free energy. The left, middle and right of this figure correspond to the systems of the three energy items in Eq. (18). **c** Physical image of the impurity-vacancy binding Gibbs free energy. The four pictures in this figure correspond to the systems of four energy items in Eq. (20)



q is the charge carried by the defects. In this study, a system with only one vacancy and a charge of 0 is considered.

Therefore, the vacancy formation Gibbs free energy ΔG_{1V}^F can be rewritten as

$$\Delta G_{1V}^F = G_{1V} - G_{bulk} + \mu_{atom} \tag{18}$$

where G_{1V} is the Gibbs free energy for a crystal containing only one vacancy and μ_{atom} is the atomic potential of the removed atom in the crystal.

Both Fig. 1b and Eq. (18) show that there are no terms related to the mass of the impurity atoms. Therefore, ΔG_{1V}^F is the same before and after replacing the light and heavy isotopes of the impurity atoms. Similar to the case of *f*, although the influence of ΔG_{1V}^F in *D* cannot be neglected, its influence on the isotope effect of vacancy-mediated impurity diffusion can be canceled. It can be expressed as

$$\frac{\exp\left(-\frac{\Delta G_{1V}^F}{k_B T}\right)^*}{\exp\left(-\frac{\Delta G_{1V}^F}{k_B T}\right)} = 1 \tag{19}$$

2.3 Impurity-vacancy binding Gibbs free energy (ΔG_{X-V}^B)

Crystal defects are not only impurities or vacancies alone, impurity-vacancy pairs can also coexist. In this case, we need to consider the interaction between impurities and vacancies, and the Gibbs free energy of binding ΔG_{X-V}^B can be defined as (Ohnuma et al. 2009)

$$\Delta G_{X-V}^B = G_X + G_{1V} - G_{X-V} - G_{bulk} \tag{20}$$

where G_X is the Gibbs free energy of the system with only one replacement impurity, and G_{X-V} is the Gibbs free energy of the system with a replacement impurity and a vacancy in its immediate neighborhood.

In Fig. 1c, G_{X-V} and G_X are associated with the impurity atoms, which means that they might change after the light and heavy isotopes of the impurity atoms are replaced. Therefore, we can derive the following equation:

$$\frac{\exp\left(\frac{\Delta G_{X-V}^B}{k_B T}\right)^*}{\exp\left(\frac{\Delta G_{X-V}^B}{k_B T}\right)} = \frac{\exp\left(\frac{G_X}{k_B T}\right)^* \exp\left(\frac{G_{X-V}}{k_B T}\right)}{\exp\left(\frac{G_X}{k_B T}\right) \exp\left(\frac{G_{X-V}}{k_B T}\right)^*} \tag{21}$$

2.4 Equation of the isotope effect of vacancy-mediated impurity diffusion $DIE_{(v)}$

Inspired by the method of calculating isotope equilibrium fractionation coefficients (Bigeleisen and Mayer 1947; Urey 1947), we transfer the energy terms involving the isotope effects into the partition function (*Q*) and then transform *Q* into the vibration frequencies of related isotope-substituted compounds. We ignore the volume change (ΔV) caused by the substitution of isotopes. The relationship between the Gibbs free energy (*G*) and *Q* is

$$G = F + P\Delta V \approx F = -RT \ln Q \tag{22}$$

where *F* is the Helmholtz free energy. The total *Q* of solids is composed of the electron partition function Q_{elec} and vibrational partition function Q_{vib} of the system, so,

$$Q = Q_{elec} \cdot Q_{vib} \tag{23}$$

Q_{elec} are not significantly different for heavy and light isotopes. Then, we can deduce that

$$\frac{\exp\left(\frac{\Delta G_{X-V}^B}{k_B T}\right)^*}{\exp\left(\frac{\Delta G_{X-V}^B}{k_B T}\right)} = \frac{\left(\frac{Q_{vib}^*}{Q_{vib}}\right)_{X-V}^{IS}}{\left(\frac{Q_{vib}^*}{Q_{vib}}\right)_X^{IS}} \quad (24)$$

Combining Eq. (16), Eq. (19) and Eq. (21), Eq. (9) can be expressed as

$$\frac{D^*}{D} = \left(\frac{v^*}{v}\right)_{X-V}^{TS} \frac{\left(\frac{Q_{vib}^*}{Q_{vib}}\right)_{X-V}^{TS}}{\left(\frac{Q_{vib}^*}{Q_{vib}}\right)_{X-V}^{IS}} \cdot \frac{\left(\frac{Q_{vib}^*}{Q_{vib}}\right)_{X-V}^{IS}}{\left(\frac{Q_{vib}^*}{Q_{vib}}\right)_X^{IS}} = \left(\frac{v^*}{v}\right)_{X-V}^{TS} \cdot \frac{\left(\frac{Q_{vib}^*}{Q_{vib}}\right)_{X-V}^{TS}}{\left(\frac{Q_{vib}^*}{Q_{vib}}\right)_X^{IS}} \quad (25)$$

where Q_{vib} is only related to the harmonic vibration frequencies (ν) (McQuarrie and Simon 1999), and Eq. (25) can be expanded by

$$\frac{D^*}{D} = \left(\frac{u^*}{u}\right)_{X-V}^{TS} \cdot \left[\prod_i^{3N} \frac{\exp\left(-\frac{u_i^*}{2}\right)}{\exp\left(-\frac{u_i}{2}\right)} \cdot \frac{1 - \exp(-u_i)}{1 - \exp(-u_i^*)} \right]_{X-V}^{TS} \cdot \left[\prod_i^{3N} \frac{\exp\left(-\frac{u_i}{2}\right)}{\exp\left(-\frac{u_i^*}{2}\right)} \cdot \frac{1 - \exp(-u_i^*)}{1 - \exp(-u_i)} \right]_X^{IS} \quad (26)$$

This is the equation for the isotope effect in vacancy diffusion for impurity atoms. where $u = \frac{h\nu}{k_B T}$, ν is the harmonic vibration frequency, X and V in the subscript of the equation denote the impurity and the vacancy, respectively, and TS and IS in the superscript of the equation denote the transition state and initial structure, respectively. N is the number of atoms in the supercells of interest. Although the equation is complicated, all the parameters are the vibration frequencies of the impurity atoms and the surrounding system. The $DIE_{(v)}$ can be easily calculated as long as the frequencies are obtained. Here, the vibration frequencies are obtained by first-principles calculations.

2.5 Calculation details

Based on density functional theory (DFT), all calculations used the Vienna Ab initio Simulation Package (VASP) (Kresse and Hafner 1993; Kresse and Furthmüller 1996) to obtain crystal parameters and vibration frequencies. We selected the projected augmented wave (PAW) (Blöchl 1994; Kresse and Joubert 1999) to study the Coulomb interaction energy in these systems. The exchange–correlation functional under the generalized gradient approximation (GGA) of Perdew–Burke–Ernzerhof (PBE) (Perdew et al. 1996) was used. This study selects $2 \times 2 \times 2$ Cu supercells and Au supercells as the calculation systems and ^{199}Au , ^{195}Au , ^{60}Co ,

and ^{57}Co as impurity atoms. The plane-wave energy cutoff of the Cu supercell was set to 400 eV and that of the Au supercell was set to 380 eV. The climbing image nudged elastic band method (CI-NEB) was used (Henkelman et al. 2000, 2002; Henkelman and Jónsson 2000) to search for transition states during the diffusion processes. Structure optimization was implemented before performing the CI-NEB calculations, and a frequency calculation was also implemented for every optimized structure. We chose an EDIFFG value of -0.001 eV/Å in this study to obtain results with acceptable accuracy and precision.

3 Results

3.1 Equation of the isotope effect of vacancy-mediated impurity diffusion $DIE_{(v)}$

Based on statistical mechanics, we obtained the general equation for the isotope effect of vacancy-mediated impurity diffusion $DIE_{(v)}$, which is expressed by Eq. (26). The $DIE_{(v)}$ can be easily calculated as long as the frequencies of the impurity atoms and the surrounding system are provided. Moreover, the vibration frequency can be obtained by first-principles calculations.

3.2 Tested systems

To test the accuracy of Eq. (26), we calculated the $DIE_{(v)}$ of $^{199}\text{Au}/^{195}\text{Au}$ and $^{60}\text{Co}/^{57}\text{Co}$ in Cu and Au metals (Fig. 2), which have well-constrained experimental data. Figure 3 and Table 1 show the $DIE_{(v)}$ for the four test systems and comparisons with the experimental data. At 1130 K and 1138 K, the D^*/D of ^{60}Co and ^{57}Co in the Cu crystal is approximately

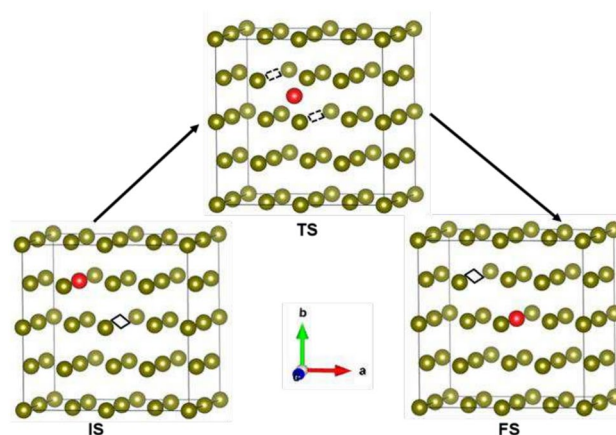


Fig. 2 Schematic diagram of the vacancy diffusion for impurity atoms (Au or Co) in a metal crystal (Cu or Au). Black boxes represent vacancies, red balls represent impurity atoms, and green balls represent solvent atoms

Fig. 3 Comparison of the experimental results (D^*/D) and those calculated by using the method provided in this study. The stars represent the values obtained in this study, and the solid dots represent the experimental values. ^{64}Cu was selected as the main component of Cu, and ^{197}Au was selected as the main component of Au. Therefore, ^{195}Au and ^{199}Au can be regarded as impurities. ^aFrom Neumann 1987. ^bFrom Herzig et al. 1978

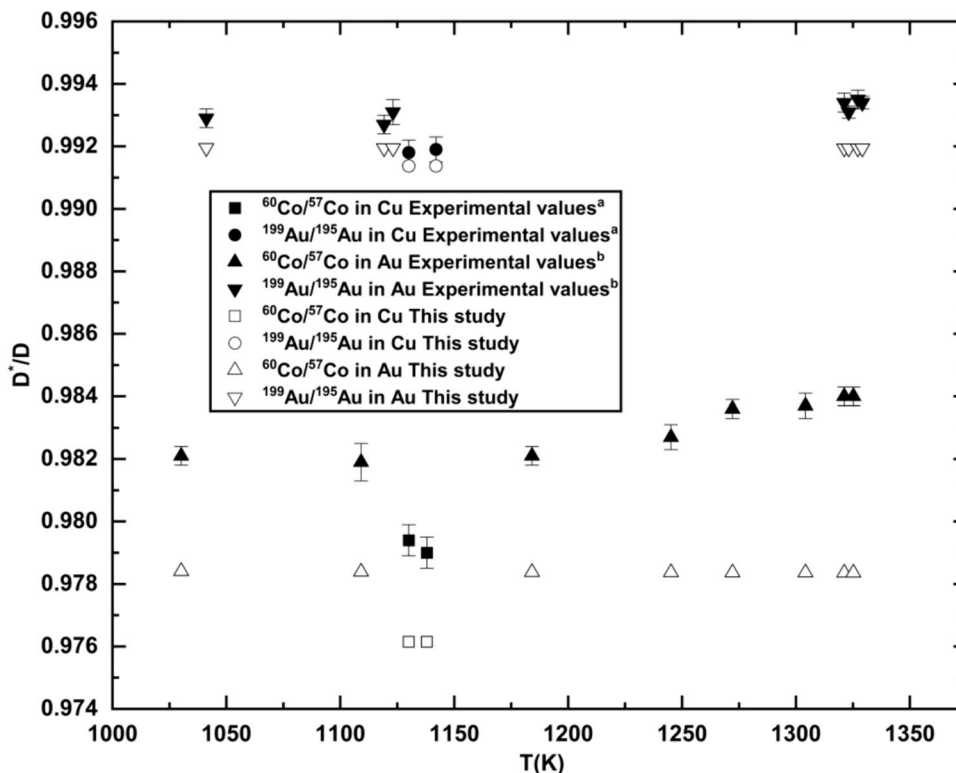


Table 1 Comparison of D^*/D between the experimental and our results

Tracer	T/K	$[D^*/D]_{(Exp.)}$	$[D^*/D]_{(This\ study)}$
$^{60}\text{Co}/^{57}\text{Co}$ in Cu	1130	0.9794 ± 0.0005^a	0.9761507
$^{60}\text{Co}/^{57}\text{Co}$ in Cu	1138	0.9790 ± 0.0005^a	0.9761510
$^{199}\text{Au}/^{195}\text{Au}$ in Cu	1130	0.9918 ± 0.0004^a	0.9913753
$^{199}\text{Au}/^{195}\text{Au}$ in Cu	1142	0.9919 ± 0.0004^a	0.9913755
$^{60}\text{Co}/^{57}\text{Co}$ in Au	1030.15	0.9821 ± 0.0003^b	0.9784058
$^{60}\text{Co}/^{57}\text{Co}$ in Au	1109.15	0.9819 ± 0.0006^b	0.9783902
$^{60}\text{Co}/^{57}\text{Co}$ in Au	1184.15	0.9821 ± 0.0003^b	0.9783781
$^{60}\text{Co}/^{57}\text{Co}$ in Au	1245.15	0.9827 ± 0.0004^b	0.9783699
$^{60}\text{Co}/^{57}\text{Co}$ in Au	1272.15	0.9836 ± 0.0003^b	0.9783666
$^{60}\text{Co}/^{57}\text{Co}$ in Au	1304.15	0.9837 ± 0.0004^b	0.9783630
$^{60}\text{Co}/^{57}\text{Co}$ in Au	1321.15	0.9840 ± 0.0003^b	0.9783612
$^{60}\text{Co}/^{57}\text{Co}$ in Au	1325.15	0.9840 ± 0.0003^b	0.9783608
$^{199}\text{Au}/^{195}\text{Au}$ in Au	1041.15	0.9929 ± 0.0003^b	0.9919534
$^{199}\text{Au}/^{195}\text{Au}$ in Au	1119.15	0.9927 ± 0.0003^b	0.9919481
$^{199}\text{Au}/^{195}\text{Au}$ in Au	1123.15	0.9931 ± 0.0004^b	0.9919478
$^{199}\text{Au}/^{195}\text{Au}$ in Au	1321.15	0.9934 ± 0.0003^b	0.9919384
$^{199}\text{Au}/^{195}\text{Au}$ in Au	1323.15	0.9931 ± 0.0002^b	0.9919383
$^{199}\text{Au}/^{195}\text{Au}$ in Au	1327.15	0.9935 ± 0.0003^b	0.9919382
$^{199}\text{Au}/^{195}\text{Au}$ in Au	1329.15	0.9934 ± 0.0002^b	0.9919381

^aFrom Eckseler and Herzig 1978. ^bFrom Herzig et al. 1978. Since several experiments were conducted at the same temperature, the average values of the experimental results were selected in this work for comparison (For example, the first four rows in Table 1)

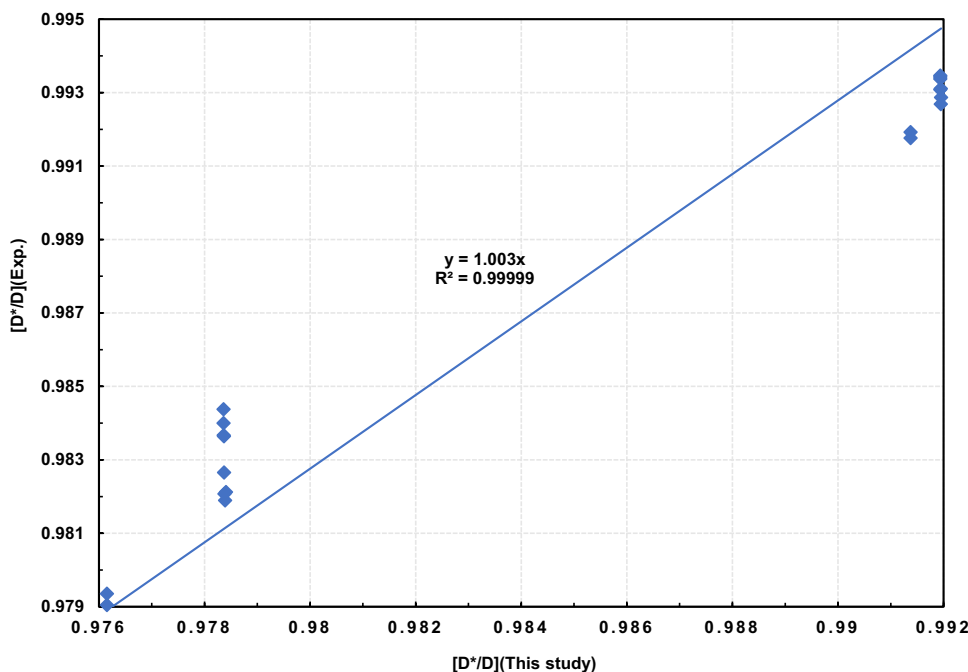
0.976, and the experimental value (Eckseler and Herzig 1978) is approximately 0.979. The difference between this study and the experimental values is 0.27%–0.37%. At 1130 K and 1142 K, the D^*/D of ^{195}Au and ^{199}Au in the Cu crystal is approximately 0.9914, the experimental value (Eckseler and Herzig 1978) is approximately 0.9916–0.9919, and the difference is 0.02%–0.06%. At the corresponding temperature, the difference between 60 and ^{57}Co in Au crystals between this study and the experimental values (Herzig et al. 1978) is 0.35%–0.57%, and the difference between 195 and ^{199}Au in Au crystals is 0.07%–0.17%. Using the data presented in Table 1, we compared our calculations and experimental D^*/D values in Fig. 4. The resulting plot exhibits a straight line passing through the origin, with an R^2 value of 0.99999 and a slope of 1.003. This observation suggests that the predicted D^*/D values are slightly underestimated by 0.3% compared to the experimental results. This close agreement indicates that Eq. (26) is both reasonable and precise.

4 Discussion

4.1 Comparison of the experimental and calculated results

The slight discrepancy between the experimental results and the calculated results is readily comprehensible. It has been suggested that D^*/D measured in the experimental process

Fig. 4 Experimental plot of D^*/D versus the calculated D^*/D in this study



is the result of various diffusion mechanisms acting together (Mehrer and Seeger 1970; Mehrer 1978; Peterson 1978; Wollenberger 1983). Seeger and Mehrer (Mehrer and Seeger 1970) reported that divacancies ($2V$) might be produced and that their concentration will increase with increasing temperature, especially when the temperature approaches the $2/3$ melting point temperature (T_m) (Mehrer 1978; Peterson 1978). It is important to note that not all metal divacancy contributions become significant (greater than monovacancy contributions) when $T > 2/3T_m$. The contribution of divacancy varies for different metals at higher temperatures, and at least at temperatures below $2/3T_m$, vacancy diffusion in most metals is dominated by a monovacancy (Mehrer 2007).

A divacancy consists of two monovacancies on nearest-neighbor lattice sites. In a real diffusion process, both monovacancy diffusion ($1V$) and divacancy diffusion ($2V$) proceed at the same time. The total diffusivity of the impurity atom is the sum of their contributions. Here,

$$C_{total} = C_{1V} + C_{2V} \tag{27}$$

the C_{total} denotes the sum of contributions of all diffusion mechanisms, and the subscript indicates a specific diffusion mechanism.

For the four experimental systems selected in this paper, the divacancy contribution C_{2V} for the diffusion processes of $^{60}\text{Co}/^{57}\text{Co}$ in Cu, $^{60}\text{Co}/^{57}\text{Co}$ in Au, and $^{199}\text{Au}/^{195}\text{Au}$ in Au have been investigated experimentally (Ecksele and Herzig 1978; Herzig et al. 1978; Neumann 1987), regardless of their proportion, and showed that the diffusion process is dominated by a monovacancy at and

below the melting point. Figure 3 shows the comparisons of the experimental results and those calculated in this study. The experimental values agree well with our theoretical calculations, which proves the diffusion process is dominated by the monovacancy mechanism because our theoretical model is a specific monovacancy mechanism. The slight discrepancy in Fig. 3 was found at higher temperatures, which reveals the transformation of the diffusion mechanism at high temperatures, where the contribution of the divacancy mechanism increases. Perhaps there are other diffusion mechanisms, such as grain-boundary and dislocation-pipe diffusion.

On the other hand, we can roughly estimate the contribution of the divacancy mechanism or other mechanism to the whole diffusion process in a certain temperature range if the isotope effect (D^*/D) under each diffusion mechanism is used as an assessment of the contribution of the mechanism, then the C_{2V} can also be expressed by:

$$C_{2V} = \frac{\left| \left(\frac{D^*}{D} - 1 \right)_{\text{experimental}} - \left(\frac{D^*}{D} - 1 \right)_{\text{thisstudy}} \right|}{\left(\frac{D^*}{D} - 1 \right)_{\text{experimental}}} \tag{28}$$

Table 2 shows the C_{2V} for the diffusion processes of $^{60}\text{Co}/^{57}\text{Co}$ in Cu, $^{60}\text{Co}/^{57}\text{Co}$ in Au, and $^{199}\text{Au}/^{195}\text{Au}$ in Au (Ecksele and Herzig 1978; Herzig et al. 1978; Neumann 1987), are approximately 13%–19%, 20%–33%, and 10%–28%, respectively at experimental temperatures. The calculated values of C_{2V} based on Eq. (28) are all within the range of experimental estimation (Herzig et al. 1978;

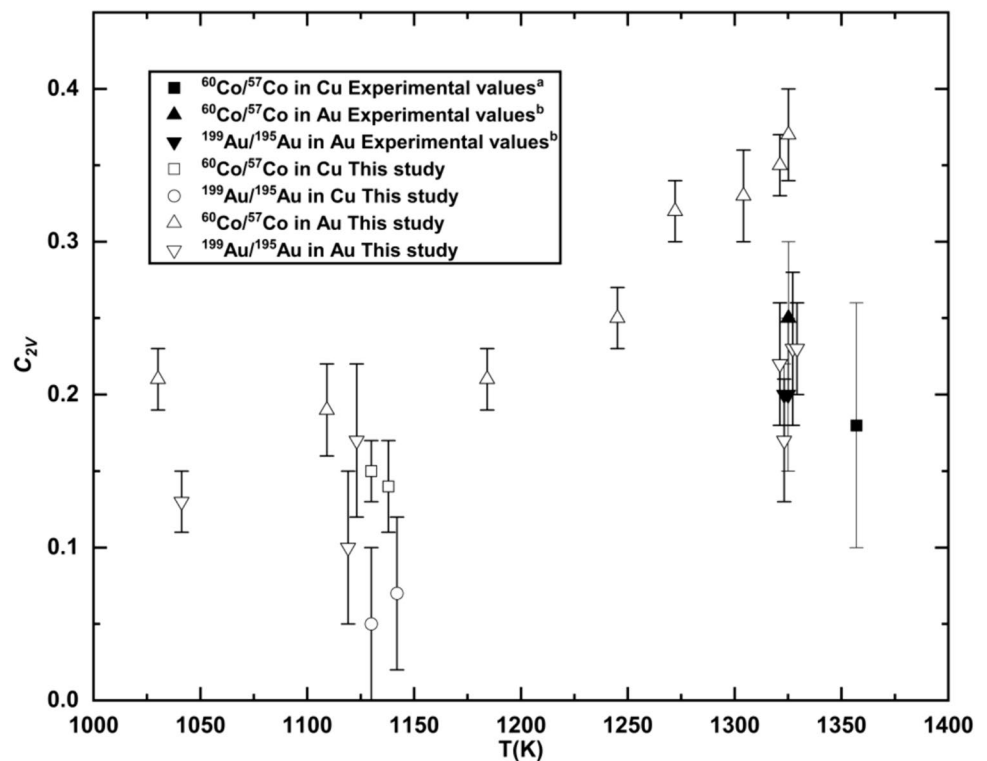
Table 2 Contribution value C_{2V} of the divacancy mechanism for the four systems

Tracer	T/K	$[C_{2V}]_{(Exp.)}$	$[C_{2V}]_{(This\ study)}$
$^{60}Co/^{57}Co$ in Cu	1130		0.15 ± 0.02
$^{60}Co/^{57}Co$ in Cu	1138		0.14 ± 0.03
$^{60}Co/^{57}Co$ in Cu	1357	0.18 ± 0.08^a	
$^{199}Au/^{195}Au$ in Cu	1130		0.05 ± 0.05
$^{199}Au/^{195}Au$ in Cu	1142		0.07 ± 0.05
$^{60}Co/^{57}Co$ in Au	1030.15		0.21 ± 0.02
$^{60}Co/^{57}Co$ in Au	1109.15		0.19 ± 0.03
$^{60}Co/^{57}Co$ in Au	1184.15		0.21 ± 0.02
$^{60}Co/^{57}Co$ in Au	1245.15		0.25 ± 0.02
$^{60}Co/^{57}Co$ in Au	1272.15		0.32 ± 0.02
$^{60}Co/^{57}Co$ in Au	1304.15		0.33 ± 0.03
$^{60}Co/^{57}Co$ in Au	1321.15		0.35 ± 0.02
$^{60}Co/^{57}Co$ in Au	1325.15	0.25 ± 0.05^b	0.37 ± 0.03
$^{199}Au/^{195}Au$ in Au	1041.15		0.13 ± 0.02
$^{199}Au/^{195}Au$ in Au	1119.15		0.10 ± 0.05
$^{199}Au/^{195}Au$ in Au	1123.15		0.17 ± 0.05
$^{199}Au/^{195}Au$ in Au	1321.15		0.22 ± 0.04
$^{199}Au/^{195}Au$ in Au	1323.15	$0.18-0.22^b$	0.17 ± 0.04
$^{199}Au/^{195}Au$ in Au	1325	0.20 ± 0.05^b	
$^{199}Au/^{195}Au$ in Au	1327.15		0.23 ± 0.05
$^{199}Au/^{195}Au$ in Au	1329.15		0.23 ± 0.03

^aExperiment estimated at T_m (1357 K) from Neumann 1987. ^bExperiment estimated at T_m (1325 K) from Herzigt et al. 1978

Neumann 1987), suggesting the rationality and accuracy of Eq. (26) for monovacancy mechanisms. We also estimate that the C_{2V} of ^{199}Au and ^{195}Au diffusion in Cu is approximately 2.8%–7.2% (Table 2), although there are no experimental data. Table 2 shows that under the conditions of $2/3T_m - T_m$ given in the experiment, the general trend of C_{2V} increases with increasing temperature, as shown in Fig. 5, which is also consistent with most experimental observations (Rothman et al. 1970; Lam et al. 1973; Backus et al. 1974). Therefore, the higher the temperature is, the greater the deviation of the experimental value from the theoretical value (see Table 1). Experimental diffusion is a comprehensive process, and in addition to the contribution of monovacancy diffusion, there are also contributions of divacancy and other diffusion mechanisms and experimental errors. Therefore, it is reasonable that the theoretically calculated value ($[C_{2V}]_{(This\ study)}$) is slightly larger than the experimental value ($[C_{2V}]_{(Exp.)}$) in Table 2. In theory, we can calculate the isotope effects under the monovacancy diffusion mechanism at any temperature. However, the evidence provided is limited to high-temperature conditions (Table 1), involving multiple mechanisms, mainly because there are no experimental D^*/D data at low temperatures (where the monovacancy mechanism predominates) that fit our theoretical model. The available data, albeit within a limited temperature range, demonstrate a clear correlation between lower temperatures and enhanced consistency with our calculated results. Consequently, despite the absence of direct evidence, the reliability of the model for low-temperature monovacancy

Fig. 5 Comparison of experimental values $[C_{2V}]_{(Exp.)}$ and those calculated $[C_{2V}]_{(This\ study)}$ by using the method provided in this study. ^aFrom Neumann 1987. ^bFrom Herzigt et al. 1978



mechanisms is inherently evident. In addition, the objective of this study is to develop quantitative theoretical equations that can predict data at low temperatures, thereby facilitating subsequent practical applications. It is worth noting that many solid systems in the geosciences are far below the T_m . Therefore, the monovacancy theoretical method provided here is meaningful for many related scientific issues.

4.2 Energy analysis

Figure 6 shows the trend of D^*/D with temperature. The D^*/D values of all systems are less than 1, where the D values of light isotopes are greater than those of heavy isotopes. With increasing temperature, the D^*/D for different systems shows different trends, which is very different from the interstitial mechanism. We will explain this phenomenon from an energy perspective. In interstitial diffusion, the activation energy during interstitial diffusion contains only the migration energy (Li et al. 2023), while the activation energy in vacancy diffusion contains not only the migration energy but also the binding energy and vacancy formation energy.

According to Eq. (25), the two major energy terms (isotope migration energy ratio $\left(\frac{D^*}{D}\right)_M$ and isotope binding energy ratio $\left(\frac{D^*}{D}\right)_B$) related to the isotope effect are ΔG^M and ΔG_{X-V}^B , so we divide the equation into two parts:

$$\frac{D^*}{D} = \left(\frac{v^*}{v}\right)_{X-V}^{TS} \frac{\left(\frac{Q_{vib}^*}{Q_{vib}}\right)_{X-V}^{TS}}{\left(\frac{Q_{vib}^*}{Q_{vib}}\right)_{X-V}^{IS}} \cdot \frac{\left(\frac{Q_{vib}^*}{Q_{vib}}\right)_{X-V}^{IS}}{\left(\frac{Q_{vib}^*}{Q_{vib}}\right)_X^{IS}} = \left(\frac{D^*}{D}\right)_M \left(\frac{D^*}{D}\right)_B \tag{29}$$

where ΔG^M is the migration Gibbs free energy, ΔG_{X-V}^B is the binding Gibbs free energy, and Q_{vib} is the vibrational partition function, and

$$\begin{aligned} \left(\frac{D^*}{D}\right)_M &= \left(\frac{v^*}{v}\right)_{X-V}^{TS} \frac{\left(\frac{Q_{vib}^*}{Q_{vib}}\right)_{X-V}^{TS}}{\left(\frac{Q_{vib}^*}{Q_{vib}}\right)_{X-V}^{IS}} \\ &= \left(\frac{v^*}{v}\right)_{X-V}^{TS} \cdot \exp\left[\frac{(\Delta G^{TS} - \Delta G^{IS}) - (\Delta G^{TS} - \Delta G^{IS})^*}{k_B T}\right]_{X-V} \end{aligned} \tag{30}$$

ΔG^{TS} is the Gibbs free energy of the transition state, and ΔG^{IS} is the Gibbs free energy of the initial state.

According to Eq. (24), we obtain

$$\left(\frac{D^*}{D}\right)_B = \frac{\left(\frac{Q_{vib}^*}{Q_{vib}}\right)_{X-V}^{IS}}{\left(\frac{Q_{vib}^*}{Q_{vib}}\right)_X^{IS}} = \exp\left[\frac{(\Delta G_B^* - \Delta G_B)}{k_B T}\right]_{X-V} \tag{31}$$

$(\Delta G^{TS} - \Delta G^{IS}) - (\Delta G^{TS} - \Delta G^{IS})^*$ is the difference between the light and heavy isotope migration Gibbs free energies, and $(\Delta G_B^* - \Delta G_B)$ reflects the difference between the light and heavy isotope binding Gibbs free energies.

Fig. 6 Changes in the D^*/D with temperature for $^{199}\text{Au}/^{195}\text{Au}$ in Cu (black line), $^{60}\text{Co}/^{57}\text{Co}$ in Cu (red line), $^{60}\text{Co}/^{57}\text{Co}$ in Au (blue line) and $^{199}\text{Au}/^{195}\text{Au}$ in Au (green line)

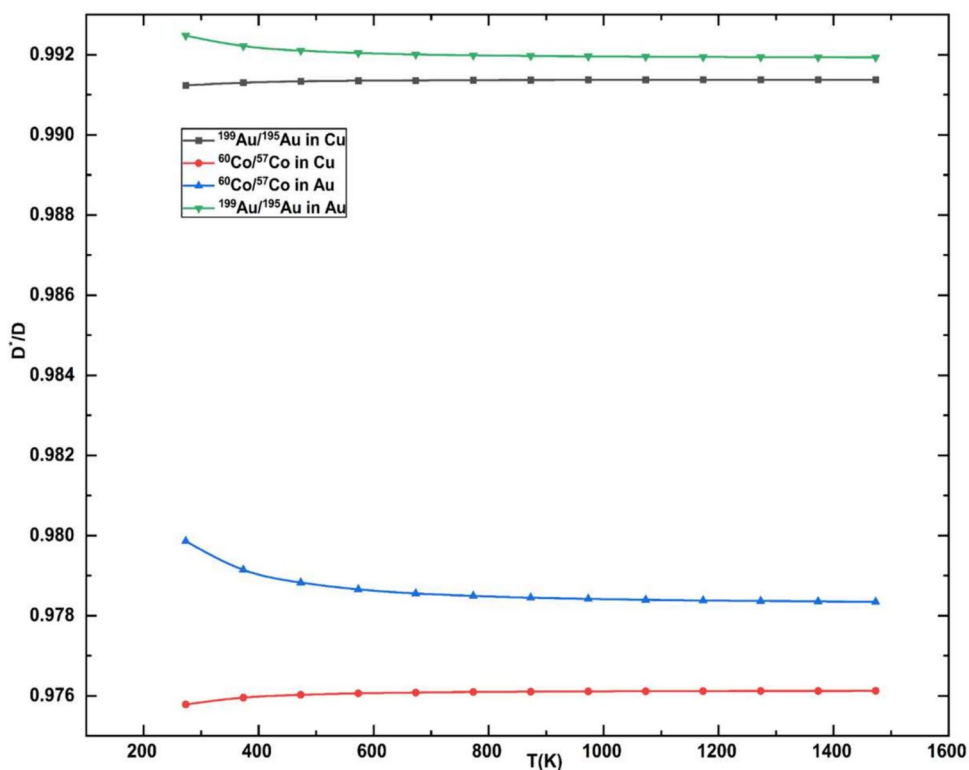


Figure 7 shows D^*/D , $(D^*/D)_M$ and $(D^*/D)_B$ for the four systems at different temperatures. The $(D^*/D)_M$ values are all less than 1, suggesting that the diffusion rate of light isotopes is faster than that of heavy isotopes. The $(D^*/D)_B$ is less than 1 or greater than 1 for different systems. If $(D^*/D)_M$ and $(D^*/D)_B$ are less than 1 (Fig. 7d), D^*/D will be much smaller than 1, so the isotope effect will increase. If $(D^*/D)_M$ is less than 1 and $(D^*/D)_B$ is greater than 1 (Fig. 7a, b and c), the migration energy and the binding energy will have opposite effects on D^*/D , and $DIE_{(v)}$ will be uncertain and depend on the system.

It is also found that $(D^*/D)_B$ has a small variation range with temperature and is close to 1 (especially in Fig. 7d),

which means that $(D^*/D)_B$ is not only slightly affected by temperature but also very little affected by the mass of light and heavy isotopes. This shows that the binding energy depends mainly on the electronic energy. However, a value close to 1 does not mean that it can be ignored. The positions of the black line and blue line are closer to each other than to the red line, which indicates that although the trend of D^*/D with temperature is the result of the combined effect of the migration energy and the binding energy, the value of D^*/D mainly depends on $(D^*/D)_M$. Therefore, the difference in migration energy for isotopes is the main driving force that determines the $DIE_{(v)}$.

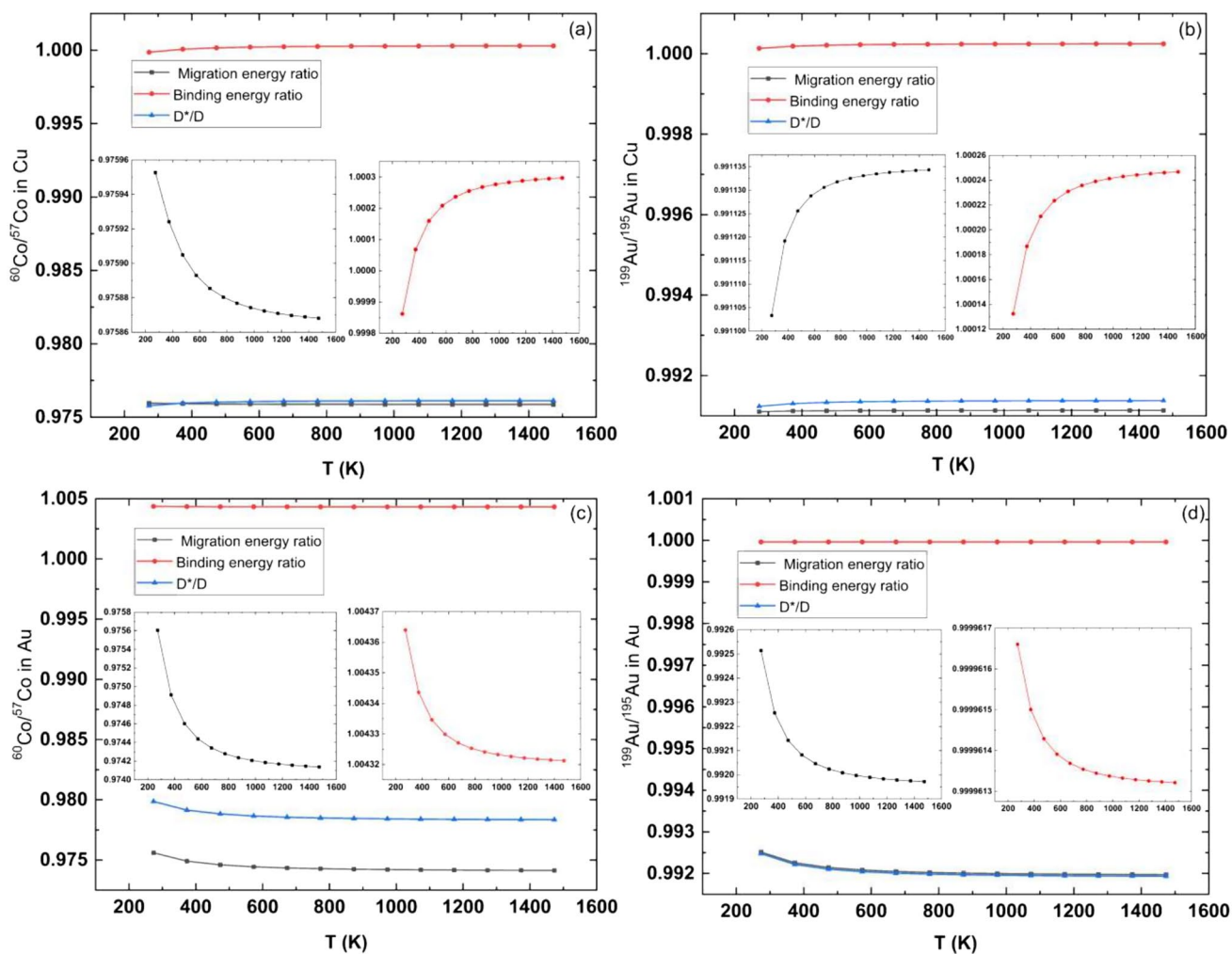


Fig. 7 Energy analysis of $(D^*/D)_M$ and $(D^*/D)_B$ for four diffusion systems at different temperatures. **a** $^{135}\text{Co}/^{57}\text{Co}$ in Cu. **b** $^{199}\text{Au}/^{195}\text{Au}$ in Cu. **c** $^{60}\text{Co}/^{57}\text{Co}$ in Au. **d** $^{199}\text{Au}/^{195}\text{Au}$ in Au. The black line represents the value of $(D^*/D)_M$, the red line represents the value of $(D^*/D)_B$, and the blue line represents the total isotope diffusion coefficient ratio (D^*/D) . The left panel shows the enlarged trend of the migration energy ratio, and the right panel shows the enlarged trend of the binding energy ratio

5 Conclusion

Based on statistical mechanics, this study built a method to calculate the isotope effect of monovacancy diffusion for impurity atoms in solids. Several important points are found:

- (1) The equation (Eq. 26) for the $DIE_{(v)}$ of impurity atoms under the monovacancy diffusion mechanism is provided, which includes only one unknown parameter: the vibration frequencies of the associated atoms and the surrounding system.
- (2) Eq. (26) is unified and can be calculated using the first-principles calculation method. The calculation results for the Co and Au systems are consistent with their experimental data, suggesting that our building theory is reasonable and can be applied to study the $DIE_{(v)}$ of monovacancy diffusion systems.
- (3) This study can estimate the weight of the contribution of other diffusion mechanisms by comparing them with the results of monovacancy diffusion, which can shed light on the mechanism of complicated diffusion processes.
- (4) From the energy analysis, this study found that the $DIE_{(v)}$ is determined by both the differences in migration energy and the binding energy for different isotopes, but the main driving force is the difference in the migration energies.

This theory will help us to understand the molecular-level mechanism of a complicated diffusion process and can be applied to materials science, solid Earth, planetary science, and any field involving solids in the future.

Author contributions X.L. and Y.L.: conceived the project; Y.J., X.L. and Y.L.: developed the method; Y.J.: performed the first-principles calculation and wrote the original draft; X.L. and Y.L.: carried out the data analysis. All the authors contributed to the interpretation of the results and editing and revising the manuscript. The project was supervised by X.L. and Y.L.

Funding This work was supported by Chinese NSF projects (42173021, 41873024, 42130114), the strategic priority research program (B) of CAS (XDB41000000), and the preresearch Project on Civil Aerospace Technologies No. D020202 funded by the Chinese National Space Administration (CNSA), and Guizhou Provincial 2021 Science and Technology Subsidies (No. GZ2021SIG).

Data availability The data supporting the main findings of this study are available in the paper. The manuscript has no associated data in a data repository. The manuscript has no data included as electronic supplementary material.

Declarations

Conflict of interest The authors declare no competing interests.

References

- Backus JGEM, Bakker H, Mehrer H (1974) Self-diffusion measurements in silver at low temperatures using single crystals and slightly deformed crystals. *Phy Stat Sol (b)* 64:151–162. <https://doi.org/10.1002/pssb.2220640119>
- Bardeen J, Herring C (1952) In imperfections in nearly perfect solids. Wiley, New York, p 262
- Bigeleisen J, Mayer MG (1947) Calculation of equilibrium constants for isotopic exchange reactions. *J Chem Phys* 15:261–267. <https://doi.org/10.1063/1.1746492>
- Blöchl PE (1994) Projector augmented-wave method. *Phys Rev B* 50:17953–17979. <https://doi.org/10.1103/PhysRevB.50.17953>
- Eckesler H, Herzig Ch (1978) On the mass dependence of the energy factor ΔK of the isotope effect for impurity diffusion in copper. *Phys Stat Sol (b)* 85:185–193. <https://doi.org/10.1002/pssb.2220850120>
- Eyring H (1935) The activated complex in chemical reaction. *J Chem Phys* 3:107–115. <https://doi.org/10.1063/1.1749604>
- Henkelman G, Jónsson H (2000) Improved tangent estimate in the nudged elastic band method for finding minimum energy paths and saddle points. *J Chem Phys* 113:9978–9985. <https://doi.org/10.1063/1.1323224>
- Henkelman G, Uberuaga BP, Jónsson HA (2000) Climbing image nudged elastic band method for finding saddle points and minimum energy paths. *J Chem Phys* 113:9901–9904. <https://doi.org/10.1063/1.1323224>
- Henkelman G, Jóhannesson G, Jónsson H (2002) Methods for finding saddle points and minimum energy paths. *Theo Meth Cond Phase Chem* https://doi.org/10.1007/0-306-46949-9_10
- Herzig C, Eckesler H, Bussmann W, Cardis D (1978) The temperature dependence of the isotope effect for self-diffusion and cobalt impurity-diffusion in gold. *J Nucl Mat* 69–70:61–69. [https://doi.org/10.1016/0022-3115\(78\)90236-2](https://doi.org/10.1016/0022-3115(78)90236-2)
- Jing Y (2022) Quantitative interpretation of isotope correlation coefficient ratios in solid diffusion. *ASIR* 6:124–128. <https://doi.org/10.22158/asir.v6n4p124>
- Kalyagin DS, Ermolenko YuE, Vlasov YuG (2008) Diffusion of Tl-204 isotope and ionic conductivity in Tl_4HgI_6 membrane material for chemical sensors. *Russ J Appl Chem* 81(12):2172–2174. <https://doi.org/10.1134/S1070427208120264>
- Kobayashi K, Hoshino T (2018) Numerical investigation for lithium isotope effect in ionic superconductor. *Fusion Eng Des* 136:205–209. <https://doi.org/10.1016/j.fusengdes.2018.01.052>
- Kresse G, Furthmüller J (1996) Efficient iterative schemes for Ab initio total-energy calculations using a plane-wave basis set. *Phys Rev B* 54:11169–11186. <https://doi.org/10.1103/PhysRevB.54.11169>
- Kresse G, Hafner J (1993) Ab initio molecular dynamics for open-shell transition metals. *Phys Rev B* 48:13115–13118. <https://doi.org/10.1103/PhysRevB.48.13115>
- Kresse G, Joubert D (1999) From ultrasoft pseudopotentials to the projector augmented-wave method. *Phys Rev B* 59:1758–1775. <https://doi.org/10.1103/PhysRevB.59.1758>
- Lam NQ, Rothman SJ, Mehrer H, Nowicki LJ (1973) Self-diffusion in silver at low temperatures. *Phy Stat Sol (B)* 57:225–236. <https://doi.org/10.1002/pssb.2220570122>
- Le Claire AD (1966) Some comments on the mass effect in diffusion. *Philos Mag* 14(132):1271–1284. <https://doi.org/10.1080/14786436608224292>
- Li X, Zhang Y, Liu Y (2023) Diffusional isotope effect based on the transition-state theory of interstitial mechanism in solids. *ACS Earth Space Chem* 7(1):28–40. <https://doi.org/10.1021/acsearthsp.acechem.2c00110>
- Lomer WM (1958) Vacancies and other point defects in metals and alloys. Institute of metals, London, p 79

- McQuarrie DA, Simon JD (1999) Molecular thermodynamics. Sterling Publishing Company, New York
- Mehrer H (1978) Atomic jump processes in self-diffusion. *J Nucl Mat.* [https://doi.org/10.1016/0022-3115\(78\)90235-0](https://doi.org/10.1016/0022-3115(78)90235-0)
- Mehrer H (2007) Diffusion in solids: fundamentals, methods, materials diffusion-controlled processes. Springer Science & Business Media, Berlin
- Mehrer H, Seeger A (1970) Interpretation of self-diffusion and vacancy properties in silver. *Phys Stat Sol (b)* 39(2):647–658. <https://doi.org/10.1002/pssb.19700390232>
- Morita K, Hoshino T (2020) Ab initio molecular dynamics study of isotope effects in lithium-ion conductors. *Sol Stat Ion* 355:115434. <https://doi.org/10.1016/j.ssi.2020.115434>
- Mueller T, Watson EB, Trail D, Wiedenbeck M, Van Orman J, Hauri EH (2014) Diffusive fractionation of carbon isotopes in γ -Fe: Experiment, models and implications for early solar system processes. *Geochim Cosmochim Acta* 127:57–66. <https://doi.org/10.1016/j.gca.2013.11.014>
- Neumann G (1987) A model for the calculation of monovacancy and divacancy contributions to the impurity diffusion in noble metals. *Phys Stat Sol (B)* 144(1):329–341. <https://doi.org/10.1002/pssb.2221440129>
- Ohnuma T, Soneda N, Iwasawa M (2009) First-principles calculations of vacancy-solute element interactions in body-centered cubic iron. *Acta Mat* 57:5947–5955. <https://doi.org/10.1016/j.actamat.2009.08.020>
- Perdew JP, Burke K, Ernzerhof M (1996) Generalized gradient approximation made simple. *Phys Rev Lett* 77:3865–3868. <https://doi.org/10.1103/PhysRevLett.78.1396>
- Peterson NL (1978) Self-diffusion in pure metals. *J Nucl Mat.* [https://doi.org/10.1016/0022-3115\(78\)90234-9](https://doi.org/10.1016/0022-3115(78)90234-9)
- Philibert J (1991) Atom Movements: Diffusion and Mass Transport in Solids. Les Ulis, France : Editions de Physique. Translated from the French by Steven J Rothman
- Richter F, Watson B, Chaussidon M, Mendybaev R, Ruscitto D (2014) Lithium isotope fractionation by diffusion in minerals. Part 1: pyroxenes. *Geochim Cosmochim Acta* 126:352–370. <https://doi.org/10.1016/j.gca.2013.11.008>
- Rothman SJ, Peterson NL, Robinson JT (1970) Isotope effect for self-diffusion in single crystals of silver. *Phy Stat Sol (B)* 39:635–645. <https://doi.org/10.1002/pssb.19700390231>
- Schoen AH (1958) Correlation and the isotope effect for diffusion in crystalline solids. *Phys Rev Lett* 1:138–140. <https://doi.org/10.1103/PhysRevLett.1.184>
- Trull TW, Kurz MD (1993) Experimental measurements of ^3He and ^4He mobility in olivine and clinopyroxene at magmatic temperatures. *Geochim Cosmochim Acta* 57(6):1313–1324. [https://doi.org/10.1016/0016-7037\(93\)90068-8](https://doi.org/10.1016/0016-7037(93)90068-8)
- Urey HC (1947) The thermodynamic properties of isotopic substances. *J Chem Soc.* <https://doi.org/10.1039/JR9470000562>
- Van de Walle CG, Neugebauer J (2004) First-principles calculations for defects and impurities: applications to III-nitrides. *J Appl Phys* 95:3851–3879. <https://doi.org/10.1063/1.1682673>
- Vineyard GH (1957) Frequency factors and isotope effects in solid state rate processes. *J Phys Chem Solids* 3(1–2):121–127. [https://doi.org/10.1016/0022-3697\(57\)90059-8](https://doi.org/10.1016/0022-3697(57)90059-8)
- Wert C (1950) Diffusion coefficient of C in α -iron. *Phys Rev* 79(4):601. <https://doi.org/10.1103/PhysRev.79.601>
- Wert C, Zener C (1949) Interstitial atomic diffusion coefficients. *Phys Rev* 76:1169–1175. <https://doi.org/10.1103/PhysRev.76.1169>
- Wollenberger HJ (1983) Point defects. Physical metallurgy 3rd. North-Holland Publishing Company, Amsterdam, p 1139
- Zhang Y, Cherniak DJ (2010) Diffusion in minerals and melts: introduction. *Rev Miner Geochem* 72(1):1–4. <https://doi.org/10.2138/rmg.2010.72.1>

Springer Nature or its licensor (e.g. a society or other partner) holds exclusive rights to this article under a publishing agreement with the author(s) or other rightsholder(s); author self-archiving of the accepted manuscript version of this article is solely governed by the terms of such publishing agreement and applicable law.